Monthly Notices
of the
ROYAL ASTRONOMICAL SOCIETY

Mon. Not. R. Astron. Soc. **426,** 108–119 (2012) doi:10.1111/j.1365-2966.2012.21678.x

Period doubling and Blazhko modulation in BL Herculis hydrodynamic models

R. Smolec* and P. Moskalik

Nicolaus Copernicus Astronomical Centre, ul. Bartycka 18, 00-716 Warsaw, Poland

Accepted 2012 July 6. Received 2012 July 5; in original form 2012 May 22

ABSTRACT

We present hydrodynamic BL Herculis type models which display a long-term modulation of pulsation amplitudes and phases. The modulation is either strictly periodic or quasi-periodic, with the modulation period and modulation pattern varying from one cycle to another. Such behaviour has not been observed in any BL Herculis variable so far; however, it is a common property of their lower luminosity siblings – RR Lyrae variables showing the Blazhko effect. These models provide support for the recent mechanism proposed by Buchler & Kolláth to explain this still mysterious phenomenon. In their model, a half-integer resonance that causes the period-doubling effect, discovered recently in Blazhko RR Lyrae stars, is responsible for the modulation of pulsation as well. Although our models are more luminous than is appropriate for RR Lyrae stars, they clearly demonstrate, through direct hydrodynamic computation, that the mechanism can indeed be operational.

Of great importance are models that show quasi-periodic modulation – a phenomenon observed in Blazhko RR Lyrae stars. Our models coupled with the analysis of the amplitude equations show that such behaviour may be caused by the dynamical evolution occurring in the close proximity of the unstable single periodic saddle point.

Key words: hydrodynamics – methods: numerical – stars: oscillations – stars: variables: general – stars: variables: RR Lyrae.

1 INTRODUCTION

Non-linear modelling is one of the key methods to study the large amplitude variability of classical pulsators: RR Lyrae stars and Cepheids. One of the notable successes of non-linear pulsation theory is the explanation of resonant effects in classical pulsators. One of the effects is the bump progression in the light/radial velocity curves of classical Cepheids pulsating in the fundamental mode (so-called Hertzsprung progression). The effect is caused by the 2:1 resonance between the fundamental mode and the second overtone, the latter mode being resonantly excited to high amplitude (e.g. Simon & Schmidt 1976; Kovács & Buchler 1989; Buchler, Moskalik & Kovács 1990; Bono, Marconi & Stellingwerf 2000). Due to resonant non-linear phase synchronization, the second overtone is not visible separately, but manifests itself as a distortion in the light/radial velocity curve. A similar effect is present in classical Cepheids pulsating in the first overtone (see e.g. Kienzle et al. 1999; Feuchtinger, Buchler & Kolláth 2000). Another interesting resonant effect, which we understand thanks to non-linear pulsation theory, is the period-doubling behaviour – alternating deep and shallow minima in the light/radial velocity curves. It is a characteristic feature of RV Tau variables, a group of pulsators often considered to be a subgroup of type II Cepheids (e.g. Wallerstein 2002; Szabados 2010). The period-doubling effect is caused by the half-integer resonances, as analysed by Moskalik & Buchler (1990). In the case of RV Tau variables, the 5:2 resonance between the fundamental mode and the second overtone is crucial. Period doubling was also discovered in Blazhko RR Lyrae stars observed with the satellite mission *Kepler* (Kolenberg et al. 2010; Szabó et al. 2010) and explained by Kolláth, Molnár & Szabó (2011) as a result of the 9:2 resonance between the fundamental mode and the ninth overtone. Recently, Soszyński et al. (2011) and Smolec et al. (2012) reported the discovery of the period-doubling effect in a BL Her-type star, demonstrating the predictive power of non-linear pulsation theory. The existence of period-doubled BL Her stars was in fact predicted 20 years earlier by Buchler & Moskalik (1992) (see also Buchler & Buchler 1994), who found the effect in their radiative hydrodynamic models. Smolec et al. (2012) confirmed that the 3:2 resonance between the fundamental mode and the first overtone is the cause of the alternations, as analysed earlier by Buchler & Moskalik (1992).

In Smolec et al. (2012) we have studied the period-doubling effect in BL Her models with our state-of-the-art convective hydrocodes (Smolec & Moskalik 2008a). During the test computations with decreased eddy viscosity, we identified a class of models

*E-mail: smolec@camk.edu.pl

showing modulation of pulsation amplitudes and phases, which is either strictly periodic or quasi-periodic. Such behaviour has not been detected in any BL Her star so far. Also, because of the strongly reduced eddy viscosity, the pulsations are violent and spurious spikes appear in the light curves. Still, the models are of great importance for the lower luminosity cousins of BL Her stars – RR Lyrae pulsators, in which more or less periodic modulation of pulsation amplitudes and phases – the Blazhko effect – is a common property (e.g. Kolenberg 2008).

The amplitude modulation in RR Lyrae stars is one of the most disturbing problems of stellar astrophysics. Although it was discovered more than a century ago (Blazhko 1907), its origin is still mysterious. Over the recent years, extensive ground-based observation campaigns (e.g. Kolenberg et al. 2006; Jurcsik et al. 2009) and high-quality and nearly continuous observations by the space missions *CoRoT* and *Kepler* allowed us to rule out the two models proposed to explain the Blazhko effect, the magnetic oblique rotator/pulsator model and the non-radial resonant rotator/pulsator model (see Kovács 2009, for a review). One of the main drawbacks of these models is the predicted clock-work modulation, while it became clear, with the advent of satellite data, that the Blazhko effect can be a very irregular phenomenon (see e.g. Guggenberger et al. 2011, 2012; Kolenberg et al. 2011). The recent idea of Stothers (2006), which assumes that modulation of turbulent convection by transient magnetic fields causes modulation of pulsation, was also questioned (Smolec et al. 2011; Molnár, Kolláth & Szabó 2012a). The discovery of the period-doubling effect in some Blazhko variables led to the new model behind the Blazhko modulation – the radial mode resonance model proposed by Buchler & Kolláth (2011). Using the amplitude equations (AEs) formalism (see e.g. Buchler & Goupil 1984), Buchler & Kolláth (2011) showed that the same resonance that causes the period-doubling effect in Blazhko variables, that is, the 9:2 resonance between the fundamental mode and the ninth overtone, can also cause either periodic or chaotic modulation of pulsation. The AEs formalism is a powerful tool to study non-linear pulsation, specifically the possible limit cycles and their stability. The nature of the computed limit cycles, however, depends on the arbitrarily assumed values of the saturation and resonant coupling coefficients, for which realistic values are too difficult to compute (see e.g. Klapp, Goupil & Buchler 1985; Nowakowski 2005). Consequently, it is not clear whether the specific solution of the AEs in which pulsation is modulated can be represented in the real stars. This must be confirmed with realistic non-linear hydrodynamic models. Attempts to find modulation of pulsation in hydrodynamic models of RR Lyrae stars have not led to success so far, likely because of the surface nature of the involved ninth-order overtone, which is difficult to model (Buchler & Kolláth 2011). In this paper, we present the hydrodynamic models of BL Her variables. These stars are more luminous siblings of RR Lyrae stars, sharing with them masses, effective temperatures and chemical composition. In these models, a low-order 3:2 resonance, between the fundamental mode and the first overtone, causes modulation of pulsation. Our calculations demonstrate for the first time that the mechanism proposed by Buchler & Kolláth (2011) can indeed be operational in hydrodynamic models. In addition, they illustrate how the quasi-periodic modulation may arise. Thus, they provide strong support for the radial mode resonance model of the Blazhko effect.

We first present our hydrodynamic models which display modulation of pulsation (Section 2) and next we demonstrate that the computed behaviour can be captured and understood with the AEs formalism (Section 3). In Section 4, we comment on the reliability of the models and on the mechanisms responsible for the wealth of detected behaviours. Finally, in Section 5, we discuss the implications of our results for understanding the Blazhko effect in RR Lyrae stars.

2 HYDRODYNAMIC MODELS

The hydrodynamic models were computed with the Warsaw non-linear, convective, pulsation codes (Smolec & Moskalik 2008a). Numerical parameters (zoning) and convective parameters, except eddy viscosity, are the same as in Smolec et al. (2012) (see their section 3.1 and table 2, set P1). The eddy viscosity (α_m parameter) was decreased from 0.25 to 0.05. The resulting fundamental mode instability strip (IS) – see Fig. 1 – is very wide; the red edge was not reached in our computations. For the first overtone we observe an additional thin IS extending to the red of the usual first overtone IS and towards the higher luminosities. Consequently, our models do not present a realistic scenario for BL Her pulsation (see Section 4 for a detailed discussion). Yet, they show a very interesting feature, namely the periodic amplitude modulation on top of the period-doubling alternations – see the bottom panel of Fig. 2 for an example. In Fig. 1, we show the location of these interesting models in the Hertzsprung–Russell (HR) diagram (horizontal line segments). Overplotted are loci of several half-integer resonances. Each of them can, in principle, cause the period-doubling effect and modulation of pulsation (Section 3; Moskalik & Buchler 1990). Although the modulation domain coincides with the loci of the 7:2 resonance with the fourth overtone, the modulation of pulsation is most likely caused by the 3:2 resonance with the first overtone, which is responsible for the period-doubling effect in BL Her models (Smolec et al. 2012). The origin of the modulation will be discussed in more detail in Section 4.

Because of the strongly decreased eddy viscosity, the models are numerically demanding. Violent pulsation requires very

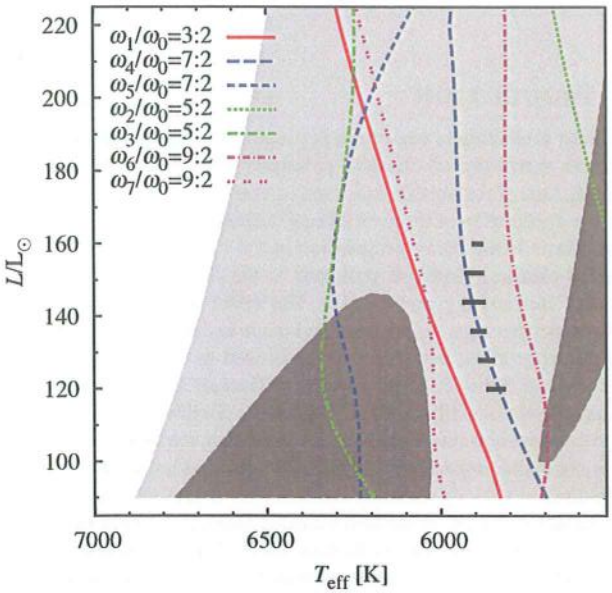

Figure 1. The HR diagram for the computed models of $M = 0.55\,M_\odot$ and $Z = 0.0001$. ISs for the fundamental mode and the first overtone are indicated with the light- and dark-shaded areas, respectively. Loci of several resonances are plotted as indicated in the key. The horizontal line segments show the domain of modulation of pulsation.

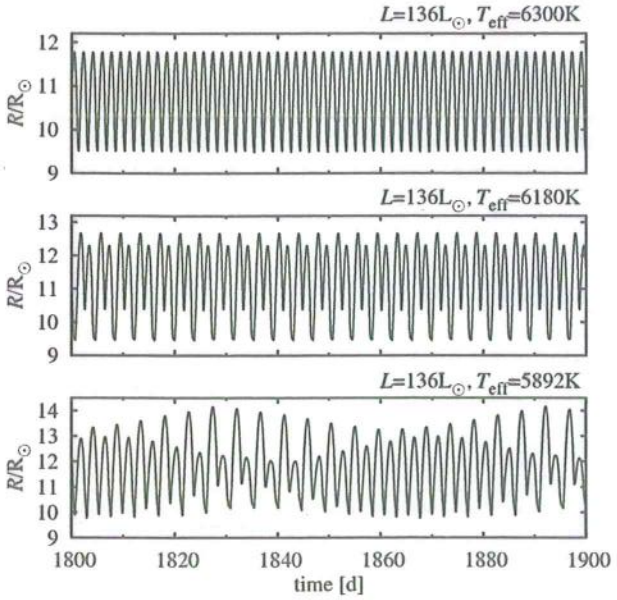

Figure 2. Radius variation for the three models of 136 $L_\odot$ and different effective temperatures.

short time-steps leading to extremely slow integration. Consequently, only a limited non-linear model survey was conducted. All models have $M = 0.55\,M_\odot$ and $Z = 0.0001$ ($X = 0.76$). We used the OP opacities (Seaton 2005) and adopted a solar mixture of Asplund et al. (2004). The non-linear models were computed along six lines of constant luminosity, $L \in \{120\,L_\odot, 128\,L_\odot, 136\,L_\odot, 144\,L_\odot, 152\,L_\odot, 160\,L_\odot\}$ and cover a limited range in effective temperatures – large enough to determine the boundaries of the domain in which the modulation of pulsation takes place. We first describe the model sequences in which all models show strictly periodic modulation of pulsation (Section 2.1). Next we describe the model sequences along which models with quasi-periodic modulation were found (Section 2.2).

2.1 Models with strictly periodic modulation of pulsation

Strictly periodic modulation was found in all models along four sequences of highest luminosity (see Fig. 1). The pulsation scenario is discussed based on the model sequence of $L = 136\,L_\odot$. The radius variation for the three models of different effective temperatures is presented in Fig. 2. The hottest model ($T_{\rm eff} = 6300$ K, top panel of Fig. 2) displays a single periodic, fundamental mode pulsation. As we decrease the model's effective temperature, the period-doubling domain emerges. The radius variation is illustrated in the middle panel of Fig. 2 for $T_{\rm eff} = 6180$ K. Alternation of radius maxima and minima is clear. At still lower effective temperatures, periodic modulation of pulsation on top of the period-doubling effect is found in the models – bottom panel of Fig. 2. The domain in which we detect this behaviour is not large; its width ≈ 50 K (see Fig. 1). To the red of this domain the period-doubling-only (no modulation) behaviour is present again, and next we find a single periodic pulsation.

The described behaviour is also clear from the analysis of the frequency spectra of the three models of Fig. 2, presented in Fig. 3. For better readability, the frequencies are normalized with the fundamental mode frequency, f_0. In the top two panels of Fig. 3, we show the frequency spectra for the two hotter models for which no modulation was detected. For single periodic pulsation in the model with $T_{\rm eff} = 6300$ K (top panel of Fig. 3), only the fundamental mode and its harmonics are present in the frequency spectrum. For the cooler model with $T_{\rm eff} = 6180$ K (middle panel of Fig. 3) a strong signal at the half-integer frequencies (subharmonics) is detected as well. It is a characteristic signature of the period-doubling effect. After pre-whitening with the fundamental mode and its harmonics ($T_{\rm eff} = 6300$ K) and subharmonics ($T_{\rm eff} = 6180$ K), we find no additional signal in the data. In the bottom panel of Fig. 3, we show the pre-whitening sequence for the model with $T_{\rm eff} = 5892$ K, which shows modulation of pulsation on top of period doubling (see the bottom panel of Fig. 2). The top panel in the pre-whitening sequence shows the frequency spectrum of the original hydrodynamic time series. The fundamental mode, its harmonic and two subharmonics are well visible. At f_0, $1/2f_0$ and at low frequencies, additional peaks are also present, which become clearly visible after pre-whitening with the fundamental mode its harmonics and subharmonics (middle panel in the pre-whitening sequence). These peaks correspond to modulation of pulsation. With the removed frequencies they form

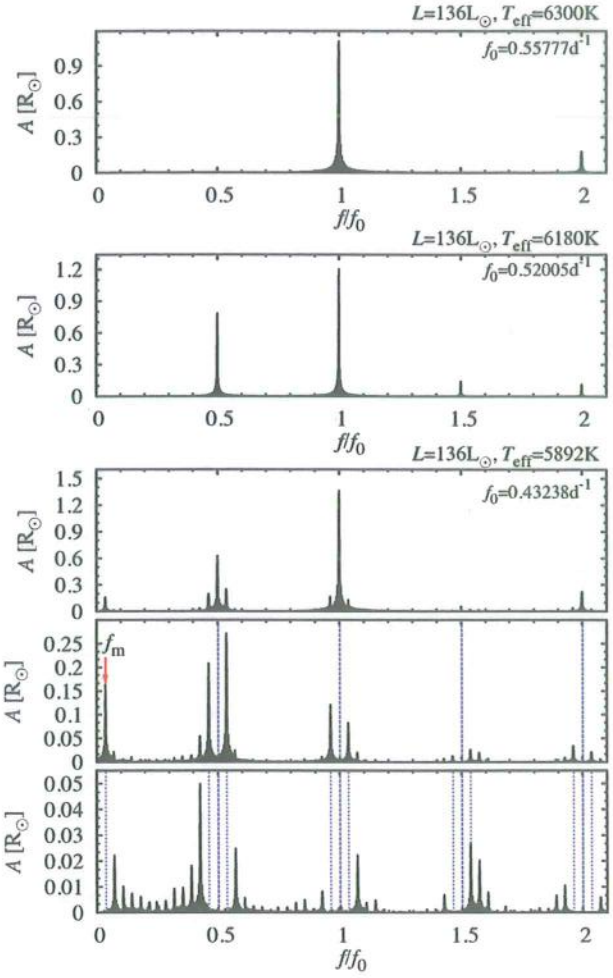

Figure 3. Frequency spectra for the models of Fig. 2. Top panel: frequency spectrum for the model with $T_{\rm eff} = 6300$ K that exhibits single periodic pulsation. Middle panel: frequency spectrum for the model with $T_{\rm eff} = 6180$ K that exhibits the period-doubling effect. Bottom panel: pre-whitening sequence for the model with $T_{\rm eff} = 5892$ K with periodic modulation of pulsation. Removed frequencies are marked with the vertical dashed lines.

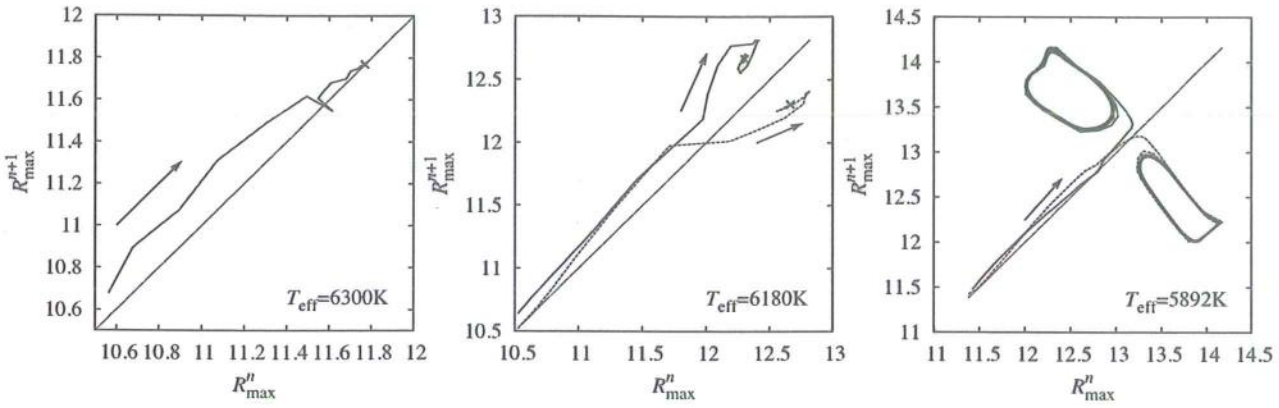

Figure 4. First return maps for radius maxima (in units of $R_\odot$) for models of Fig. 2.

the equidistant multiplets. The separation between the multiplet components corresponds to the modulation frequency, $f_{\rm m}$, which is also detected independently in the frequency spectrum. For the discussed case, the modulation period is $P_{\rm m} = 1/f_{\rm m} = 63.8$ d, which corresponds to 27.6 fundamental mode pulsation cycles.

Modulation of pulsation can also be illustrated through construction of return maps. In Fig. 4 we show the first return map for the radius maxima, that is, a plot of $R^{n+1}_{\rm max}$ versus $R^{n}_{\rm max}$, where n counts the pulsation cycles, for the three discussed models. The return maps are plotted for the full model integration, including the initial transient phase. For a single periodic model with $T_{\rm eff} = 6300$ K, after the initial transient phase, the consecutive radius maxima fall at a single point located on the diagonal (cross in the leftmost panel of Fig. 4). It corresponds to a fundamental mode limit cycle pulsation. For models with $T_{\rm eff} = 6180$ and 5892 K, which show the period-doubling effect, it is convenient to connect each second pair of radius maxima (middle and right-hand panels of Fig. 4). After the initial growth of the amplitude of single periodic pulsations, the curves constructed in this way diverge, which is a result of the increase of the period-doubling effect. For the limit cycle pulsation, the return maps for the two models are different. For the model with $T_{\rm eff} = 6180$ K, which shows the period-doubling effect and no modulation (middle panel of Fig. 4), the consecutive radius maxima alternate between two points, located symmetrically with respect to the diagonal. For the model with $T_{\rm eff} = 5892$ K, which shows periodic modulation of pulsation (right-hand panel of Fig. 4), each second pair of radius maxima follow a route along a separate loop. The modulation is strictly periodic; each loop can be described by a single curve – the broadening visible in Fig. 4 is caused by connecting with straight line segments.

The described properties of modulation are qualitatively the same for model sequences of higher luminosity, that is, for $L \in \{144\,{\rm L}_\odot, 152\,{\rm L}_\odot, 160\,{\rm L}_\odot\}$. In the upper panel of Fig. 5, we plot the modulation periods as a function of model parameters: luminosity and effective temperature. In the bottom panel, the corresponding modulation amplitude, that is, the amplitude of the highest modulation peak in the vicinity of f_0 (either $f_0 - f_{\rm m}$ or $f_0 + f_{\rm m}$), is plotted. The typical modulation periods vary from ~16 to ~35 fundamental mode pulsation cycles (45–106 d). In general, the higher the model luminosity and the higher its effective temperature, the shorter the modulation period. The modulation amplitudes decrease towards the edges of the domain in which modulation of pulsation was found. This indicates that the appearance of the modulation domain, as the model's effective temperature is changed, is a super-

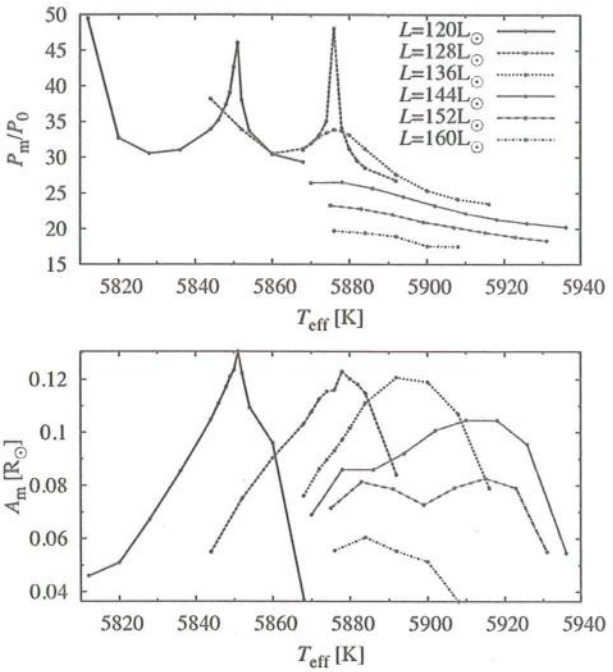

Figure 5. Modulation periods in units of the fundamental mode pulsation period (upper panel) and modulation amplitudes (bottom panel) as a function of effective temperature and luminosity (different line types).

critical bifurcation. Also, for $L \geq 136\,{\rm L}_\odot$, the higher the luminosity, the lower the modulation amplitudes. It is clear that the modulation domain shrinks towards higher luminosities and likely does not extend far beyond $160\,{\rm L}_\odot$.

In the case of the least luminous models of 120 and $128\,{\rm L}_\odot$, sharp features are clearly visible in the progression of modulation periods and amplitudes with effective temperature. These models are discussed in detail in the next section.

2.2 Models with quasi-periodic modulation of pulsation

In Fig. 6, we plot the return maps for the limit cycle pulsation (the initial transient phase was omitted) for several models along the $128\,{\rm L}_\odot$ sequence. As before, each second pair of points were connected (period doubling). For the coolest and two hottest models, the

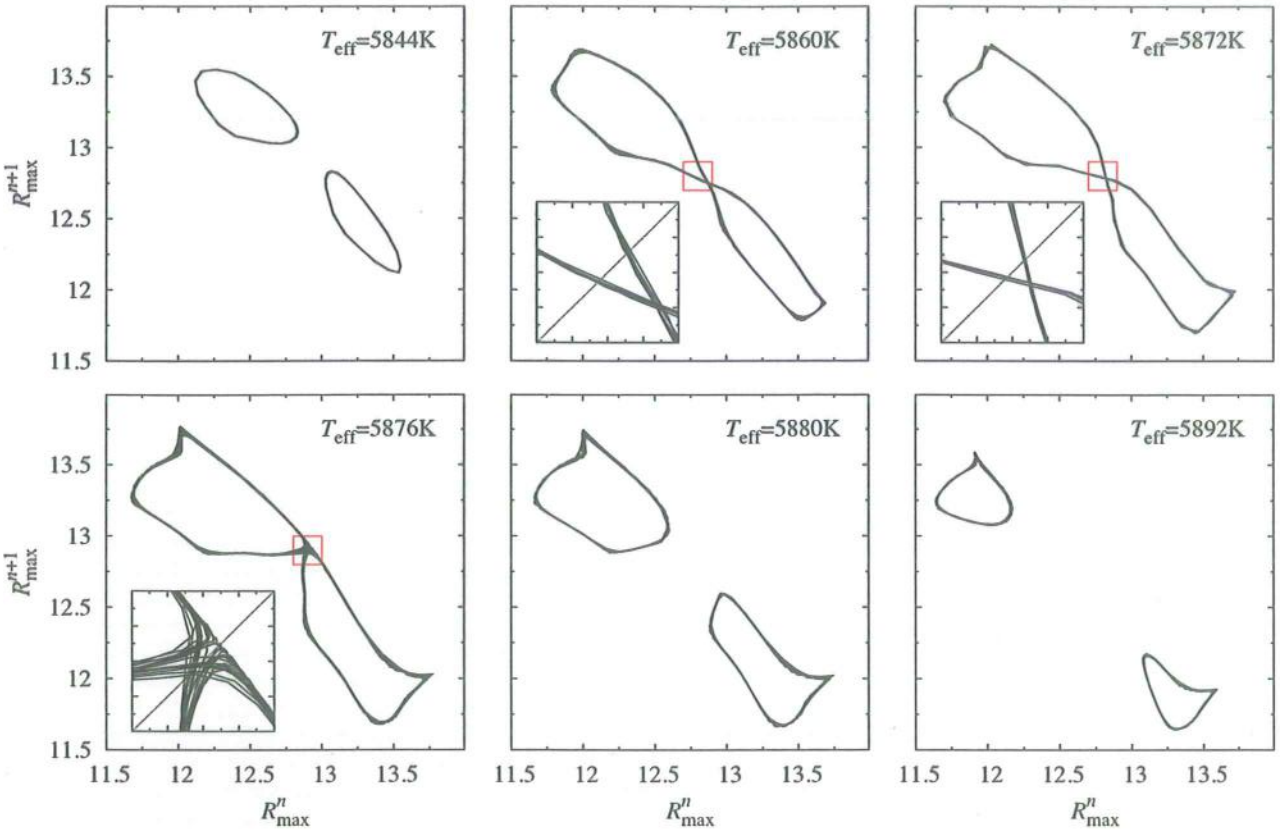

Figure 6. First return maps for maximum radii (in units of $R_\odot$) for several models with $128\,L_\odot$. The insets in the three panels show a zoom-in of the marked regions.

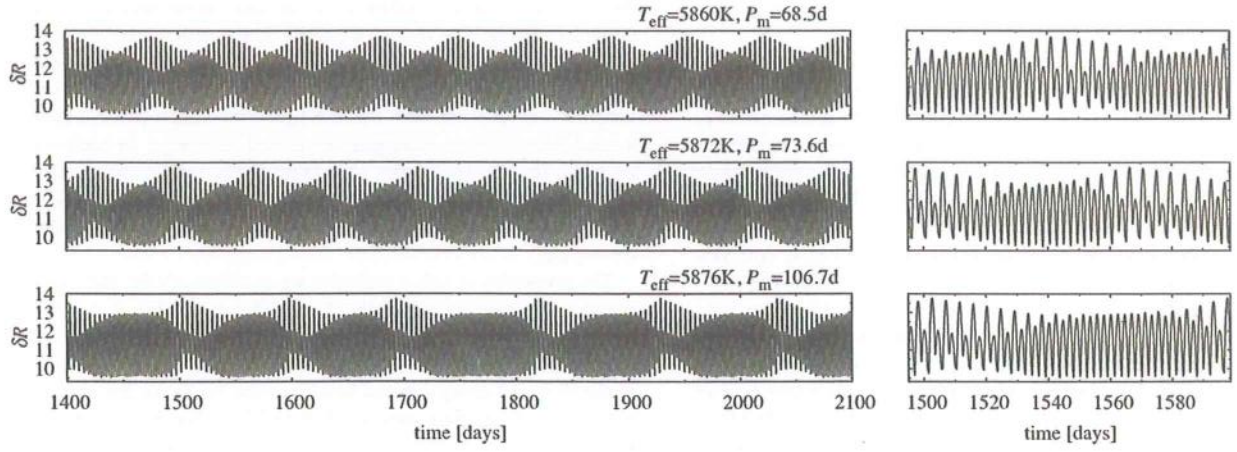

Figure 7. Radius variation for three models with $128\,L_\odot$ and different effective temperatures. The right-hand panels show a zoom-in into a 100-d segment.

return maps are qualitatively the same as discussed in the previous section (two separate loops). These models show strictly periodic modulation of pulsation. To explain the sharp increase of the modulation periods visible in Fig. 5, we focus our attention on the three models with effective temperatures of 5860, 5872 and 5876 K. Their modulation periods increase and are equal to 68.5, 73.6 and 106.7 d, respectively. The radius variation for these models is plotted in Fig. 7. The return maps have a different topology from that discussed so far. They have the shape of a figure '8'. For the two models with effective temperatures of 5860 and 5872 K, the pulsation modulation is periodic, but the higher/lower maximum pulsation cycles trade places from one modulation cycle to the other. This behaviour can be followed in Fig. 7 (in particular in the rightmost panels). Consequently, the pattern of period doubling repeats after two modulation cycles. We note that this behaviour was recently found in the *Kepler* short-cadence data for RR Lyrae (Molnár et al. 2012), although the swapping of higher/lower maximum cycles is very irregular. The frequency spectrum for the model with $T_{\rm eff} = 5872$ K

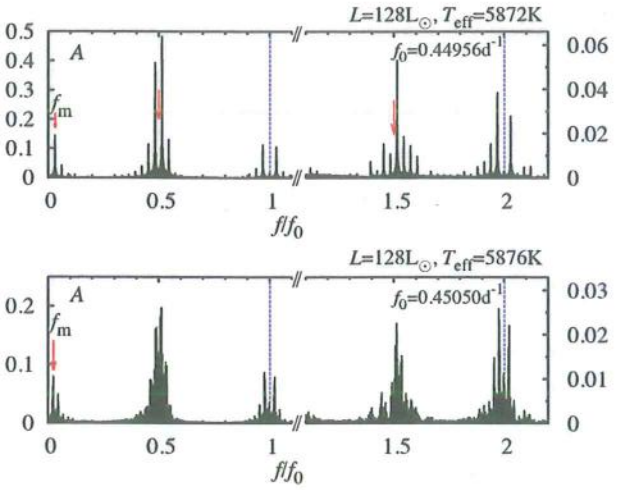

Figure 8. Frequency spectra after pre-whitening with the fundamental mode and its harmonics for two models of the 128 $L_\odot$ sequence. Note the different scales on the vertical axis on the left- and right-hand sides of the figure. Removed frequencies are marked with the dashed lines, while the arrows (top panel) show the exact location of the subharmonic frequencies, $1/2f_0$ and $3/2f_0$.

(it is qualitatively the same for the model with $T_{\rm eff} = 5860$ K), after pre-whitening with the fundamental mode and its harmonics, is plotted in the top panel of Fig. 8. At the position of the subharmonics, that is, exactly at $1/2f_0$ and $3/2f_0$, we detect no signal. Instead, a comb of equidistant frequencies, with peak separation corresponding to $f_{\rm m}$, is centred exactly on the location of the missing subharmonics. For f_0 and the harmonic frequencies (i.e. $2f_0$, $3f_0$, etc.), we observe a multiplet structure of the same properties as discussed earlier (see Fig. 3).

Even more complicated behaviour is observed for the model with $T_{\rm eff} = 5876$ K. We note that this is the model with the longest peak modulation period (Fig. 5). In fact the period of the modulation cycle, if measured from one epoch of maximum pulsation amplitude to the other, may strongly vary for this model which is well visible in the bottom panel of Fig. 7. For the plotted cycles, we estimate it to be 96, 95, 129, 106 and 107 d. The modulation is quasi-periodic. The first return map for this model is presented in Fig. 6. Analysis of the inset shows that the radius maxima either follow the route along the figure '8' or follow only its one part. As long as we continued the model integration (20 000 fundamental mode pulsation cycles, that is, more than 400 modulation cycles) no regularity could be spotted in the described behaviour. We also note that consecutive radius maxima do not follow a single curve, which is well visible in the respective inset in Fig. 6. Consequently, the modulation pattern varies from one modulation cycle to the other. This quasi-periodic behaviour is also detected in the frequency spectrum, which is plotted in the bottom panel of Fig. 8. At f_0 and its harmonic, we detect the modulation multiplet with a separation corresponding to $f_{\rm m}$. The inverse, $f_{\rm m}^{-1}$, describes the mean modulation period, which is equal to 106.7 d. At the subharmonic frequencies, broad bands of peaks with no clear structure are visible. These peaks are not coherent, contrary to the modulation peaks around f_0 and its harmonics, clearly indicating the chaotic nature of the model. Still the modulation can be described as more or less periodic, as is the case in several Blazhko RR Lyrae stars, with strongly differing modulation cycles (e.g. Guggenberger et al. 2011). We note that properties of the Fourier spectrum for the discussed model closely resemble the properties of Fourier spectra for Blazhko RR Lyrae stars showing the period-doubling effect. For these stars, bunches of peaks are present at half-integer frequencies, indicating the irregular nature of the period-doubling phenomenon (Szabó et al. 2010; Kolenberg et al. 2011).

As the models' temperature is increased beyond 5876 K, the figure '8' is broken into two separate loops (Fig. 6). Strictly periodic modulation, as described in Section 2.1, is observed again.

Analysis of the radius variation and return maps for our models provides a hint why the modulation period varies for these models (as depicted in Fig. 5) and why the modulation may become quasi-periodic. We focus our attention on the three previously discussed models (with $T_{\rm eff} = 5860$, 5872 and 5876 K), for which the radius variation is plotted in Fig. 7. During the modulation the amplitudes of the excited modes, that is, of the fundamental mode ($A(t)$ in the following) and of the resonantly coupled first overtone ($B(t)$) vary. For the three models we observe that the period doubling is quenched at some phases of the modulation cycle. It is visible in the return maps (radius maxima fall close to the diagonal, see the insets in Fig. 6), and also clearly visible in Fig. 7. The amplitude of the overtone mode must be very small then. We conclude that the model evolves in direct proximity of the point corresponding to unstable single periodic pulsation, that is, a point of $A =$ constant and $B = 0$. This unstable limit cycle corresponds to a single point on the diagonal of the return map. The topology of the return map for $T_{\rm eff} = 5876$ K (Fig. 6) suggests that it is a saddle point. The exact location of the unstable single periodic limit cycle could be determined with the help of the relaxation technique (Stellingwerf 1974). Unfortunately, it is not implemented in our code. Nevertheless, in the next section, with the help of the AEs formalism, we show that indeed the observed properties of the modulation result from the dynamical evolution close to the unstable saddle point. We will show that at a saddle point the trajectories describing the system evolution are at first attracted, but repelled later on, and that evolution is very slow (the closer the saddle point, the slower the system's evolution). Thus, the models evolving closer to the unstable saddle point have much longer modulation periods (and a much longer phase of suppressed period doubling). In addition, once the trajectories evolve very close to the saddle, the system becomes chaotic. When the system evolves far from the saddle point, the modulation is strictly periodic and occurs on a shorter time-scale.

The properties of radius variation are qualitatively the same also in our least luminous model sequence (120 $L_\odot$). In Fig. 9, we plot the return maps for three models located at the peak of modulation periods (Fig. 5). Again we observe that the radius maxima fall close to the diagonal along a broad band (see the insets for the models with effective temperatures of 5850 and 5851 K). For the model with $T_{\rm eff} = 5851$ K, the radius maxima may follow a route along the loops which approach the diagonal (and the presumed saddle point) at different distances. Corresponding modulation cycles have different lengths.

In Fig. 5, we also note a rapid increase of the modulation periods at the cool side of the modulation domain, particularly pronounced for the $L = 120\,L_\odot$ models. This increase again can be explained by the models' evolution close to the unstable saddle point.

Finally, we note that also for the 136 $L_\odot$ sequence the increase of modulation period is visible (Fig. 5) which is, however, not as prominently marked as in the case of the lower luminosity models.

We now turn to a discussion of the described modulation properties using the AEs formalism.

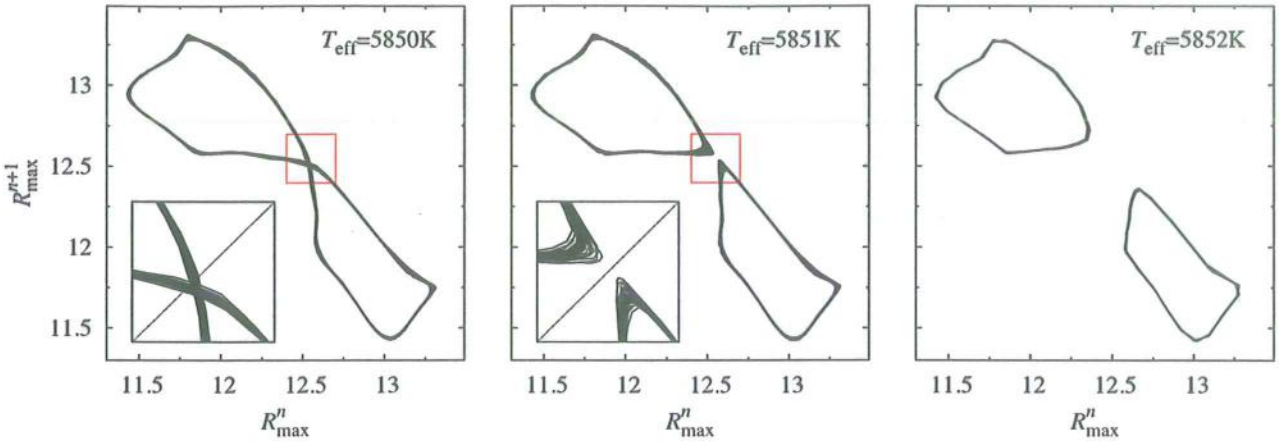

Figure 9. First return maps for maximum radii (in units of $R_\odot$) for three models with $120\,L_\odot$. The insets in the first two panels show a zoom-in of the marked regions.

3 AMPLITUDE EQUATIONS

The dynamical behaviour we have found in our models can be well captured with the AEs formalism. We follow the analysis of Buchler & Kolláth (2011), who considered the 9:2 ($9\omega_0 = 2\omega_9$) resonance responsible for the period doubling detected recently in RR Lyrae stars (Kolenberg et al. 2010; Szabó et al. 2010; Kolláth et al. 2011). All these stars show the Blazhko effect, more or less periodic modulation of the pulsation amplitude. Buchler & Kolláth (2011) showed that the same resonance is able to cause the amplitude modulation. They conducted a parametric study of the appropriate AEs and besides the fixed points they identified two types of oscillatory solutions, either strictly periodic or irregular. Here we follow their approach to study the 3:2 resonance between the fundamental mode and the first overtone which is responsible for the period-doubling effect in BL Her hydrodynamic models (Smolec et al. 2012). As noted in Section 2.1, the stable period-two cycle loses its stability and gives rise to a stable cycle in which pulsation is modulated, either periodically or quasi-periodically. Below we show that this behaviour can be captured with the AEs.

An appropriate set of complex AEs were given by Moskalik & Buchler (1990) (see also Moskalik & Buchler 1993):

$$\frac{{\rm d}a}{{\rm d}t} = ({\rm i}\omega_a + \kappa_a + Q_a|a|^2 + T_a|b|^2)\,a + c_a a^{*2} b^2\,, \tag{1a}$$

$$\frac{{\rm d}b}{{\rm d}t} = ({\rm i}\omega_b + \kappa_b + Q_b|b|^2 + T_b|a|^2)\,b + c_b a^3 b^*\,. \tag{1b}$$

The non-resonant part is truncated at the third order. Q_k and T_k are cubic, self- and cross-saturation coefficients, respectively. The last terms on the right-hand side of equations (1a) and (1b) are resonant coupling terms, with the resonant coupling coefficients c_a and c_b. These, together with complex amplitudes, are represented as $a = A{\rm e}^{{\rm i}\phi_a}$, $b = B{\rm e}^{{\rm i}\phi_b}$, $c_a = C_a{\rm e}^{{\rm i}\delta_a}$ and $c_b = C_b{\rm e}^{{\rm i}\delta_b}$, which allows us to write the above AEs as a set of three first-order differential equations with real coefficients:

$$\frac{{\rm d}A}{{\rm d}t} = \left[\kappa_a + \Re(Q_a)A^2 + \Re(T_a)B^2\right]A + C_a A^2 B^2 \cos(\Gamma + \delta_a)\,, \tag{2a}$$

$$\frac{{\rm d}B}{{\rm d}t} = \left[\kappa_b + \Re(Q_b)B^2 + \Re(T_b)A^2\right]B + C_b A^3 B \cos(\Gamma - \delta_b)\,, \tag{2b}$$

$$\frac{{\rm d}\Gamma}{{\rm d}t} = 2\Delta + [2\Im(T_b) - 3\Im(Q_a)]A^2 + [2\Im(Q_b) - 3\Im(T_a)]B^2 - 3C_a A B^2 \sin(\Gamma + \delta_a) - 2C_b A^3 \sin(\Gamma - \delta_b)\,. \tag{2c}$$

Above Γ is a combination of mode phases, $\Gamma = 2\phi_b - 3\phi_a$, and Δ is a frequency mismatch parameter,

$$\Delta = \omega_b - 3\omega_a/2\,. \tag{3}$$

Exact analytical solutions of AEs are possible only for strongly simplified cases. Moskalik & Buchler (1990) considered the AEs for half-integer resonances between the fundamental mode and the higher order overtones, $(2n+1)\omega_0 = 2\omega_k$, neglecting the cross-saturation and resonant coupling terms in the equation for the dominating fundamental mode (i.e. $T_a = 0$ and $c_a = 0$), as well as neglecting the imaginary parts of the cubic coupling coefficients. Such systems can have two non-trivial fixed points (${\rm d}A/{\rm d}t = {\rm d}B/{\rm d}t = {\rm d}\Gamma/{\rm d}t = 0$): a single-mode fixed point with non-zero amplitude of the fundamental mode only [$A = \sqrt{-\kappa_a/\Re(Q_a)}$ and $B = 0$] and a two-mode fixed point with non-vanishing amplitudes of both modes (which in general have to be derived numerically). Because of the half-integer resonance, such a solution corresponds to a period-doubled limit cycle. Oscillatory solutions for the amplitudes are possible as well and were found during the numerical integration of equations (2). To simplify the equations, we followed Buchler & Kolláth (2011) and neglected the imaginary parts of the cubic saturation coefficients. Periodic modulation of amplitudes, corresponding to hydrodynamic models described in Section 2, is relatively easy to find. We adopted the following set of saturation and coupling coefficients: $\kappa_a = 1.0$, $\kappa_b = -0.01$, $\Re(Q_a) = 1$, $\Re(Q_b) = 1.1$, $\Re(T_a) = 5.0$, $\Re(T_b) = 1.0$, $C_a = 5.75$, $C_b = 4.0$, $\delta_a = 1.95$, $\delta_b = 1.0$, and integrated the AEs with different values of Δ. These models correspond to our hydrodynamic models of different effective temperatures. The radius variation was reconstructed according to (Moskalik & Buchler 1990)

$$\delta R(t) = A{\rm e}^{{\rm i}\omega_a t} + B{\rm e}^{{\rm i}(\Gamma/2)}{\rm e}^{{\rm i}(3/2)\omega_a t} + \text{higher order terms}, \tag{4}$$

with higher order terms neglected. For the pulsation frequency, ω_a, we choose $\omega_a = 2\pi/P_a = 2\pi/0.1$ so that the relative growth rate, $\kappa_a P_a = 0.1$, is typical for BL Her models. We note that we do not expect a 1:1 equivalence between the hydrodynamic models and results of AE integration, not only because of arbitrarily assumed

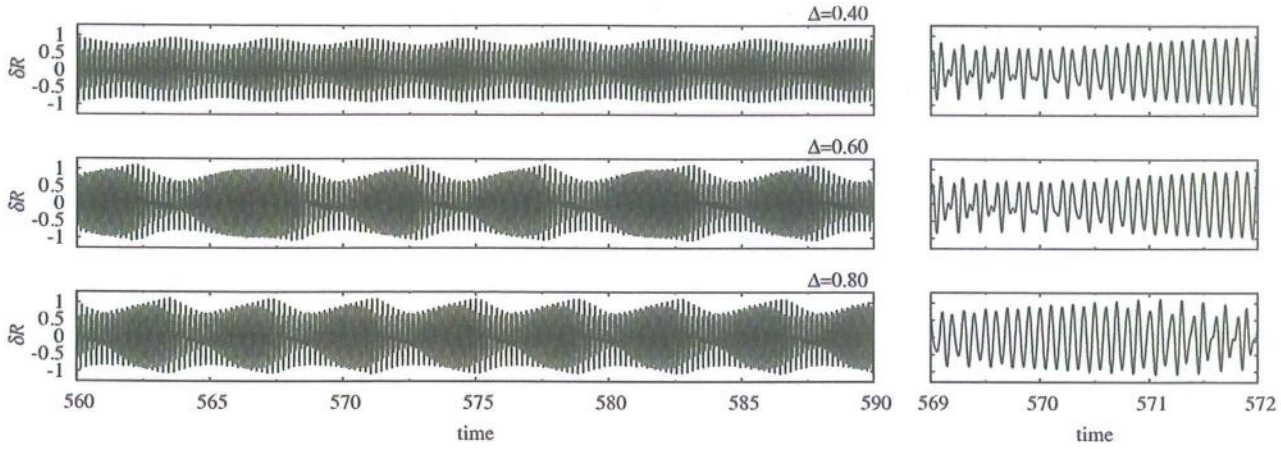

Figure 10. Radius variation for three integrations of AEs with different Δ. Note the different lengths of consecutive modulation cycles for Δ = 0.60.

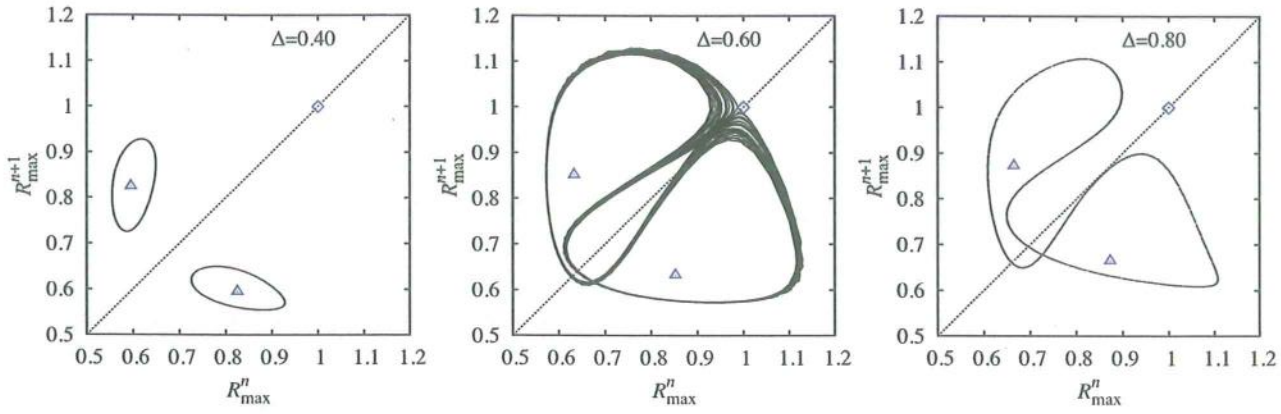

Figure 11. First return maps for radius maxima for models with different Δ. The diamond and triangles mark the locations corresponding to the unstable single-mode and two-mode fixed points, respectively.

coefficients of equations (2), but also because of neglect of the higher order terms in radius reconstruction (equation 4).

In Fig. 10 we show the radius variation for three different values of Δ. Qualitatively, the same behaviour is visible as in the hydrodynamic models (Fig. 7) – clear amplitude modulation on top of the period-doubling behaviour. The modulation is periodic for Δ = 0.4 and 0.8, and is clearly quasi-periodic for Δ = 0.6.[1] The corresponding return maps on successive radius maxima are presented in Fig. 11. The diamond and triangles mark the locations of radius maxima corresponding to the single-mode fixed point and two-mode fixed point, respectively. The fixed points are unstable as their stability eigenvalues indicate. For the single-mode point, the three eigenvalues are all real, one is positive and two are negative; thus, the single-mode fixed point is an unstable saddle point. For the two-mode fixed point, one eigenvalue is real and negative and the other two are a complex conjugate pair with positive real parts. The two-mode fixed point is thus an unstable spiral point. For models with Δ = 0.40 and 0.80, the radius maxima fall along single curves encircling the unstable two-mode fixed points and far from the unstable single-mode point. These return maps are qualitatively the same as for our hydrodynamic models that display strictly periodic modulation (e.g. the models with $T_{\rm eff} = 5844$ K or 5872 K in Fig. 6). The behaviour is very different for Δ = 0.6. The radius maxima may fall in direct proximity of the unstable single-mode point and may follow very different routes during the modulation. This is qualitatively the same behaviour as described for models with $T_{\rm eff} = 5876$ K (128 $L_\odot$) and $T_{\rm eff} = 5851$ K (120 $L_\odot$) in Section 2.2. It results from the evolution in the proximity of the unstable saddle point.

To analyse the dynamics of our models in more detail, we follow Buchler & Kolláth (2011) and consider the phase plots of amplitudes, that is, plots of $A(t)$ versus $B(t)$, which are displayed in Fig. 12 for the discussed cases. Note that the (A, B) plane is a subset of the full 3D phase-space (A, B, Γ) and that now we focus on the long-term variation, with pulsations filtered out. For Δ = 0.4 and 0.8, the phase plots are very simple – the trajectory is a single loop and the resulting modulation is strictly periodic. In the middle panel of Fig. 12, we plot the trajectories for the most interesting case of Δ = 0.6. Clearly, the trajectory is not a single curve now, which is best visible in the proximity of the unstable single-mode point ($A = 1$, $B = 0$). The phase plot indicates the presence of a strange attractor, which may be further confirmed through construction of the first return map on the consecutive maxima of amplitude $A(t)$. It is plotted in Fig. 13 and is very similar to that of the Lorentz attractor (see e.g. Bergé, Pomeau & Vidal 1984); albeit, at close inspection, it shows a double-cusp feature (see the inset). The slope

[1] The apparently large values of the mismatch parameter, Δ, result from the adopted normalization ($\kappa_a = 1$).

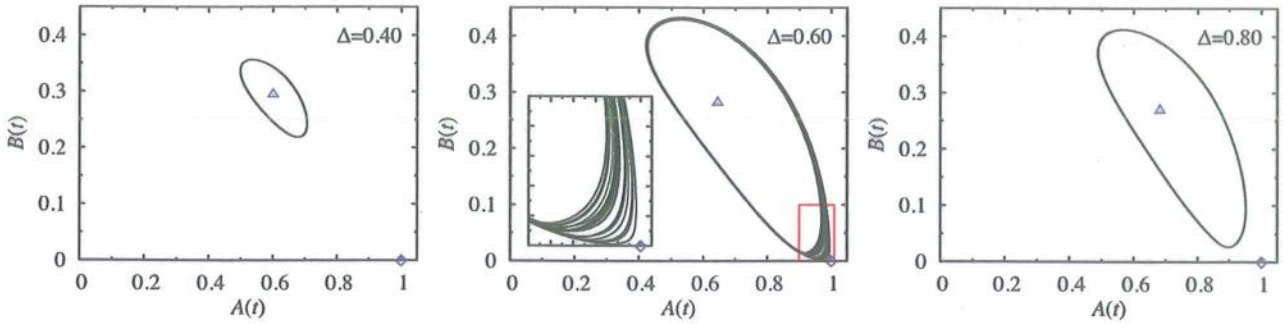

Figure 12. Trajectories in the $(A(t), B(t))$ plane for several modulation cycles and different Δ. The unstable single-mode and two-mode fixed points are marked with the diamond and triangles, respectively.

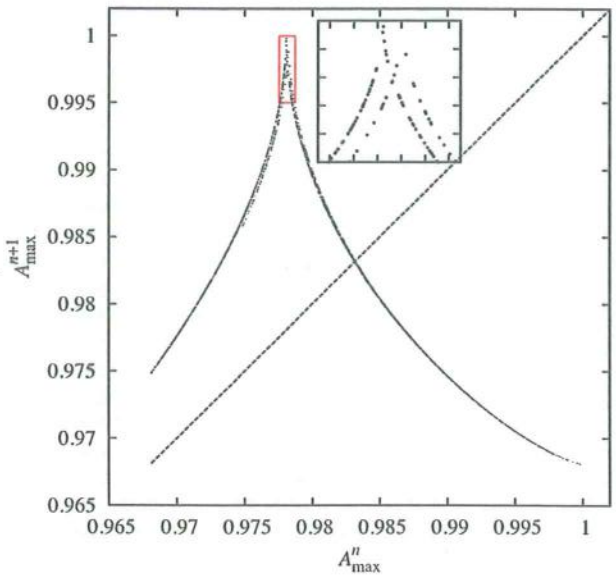

Figure 13. First return map on the successive amplitude maxima of amplitude $A(t)$: $A^{n+1}_{\max}$ versus $A^{n}_{\max}$.

of $A^{n+1}_{\max}$ versus $A^{n}_{\max}$ at the intersection with the diagonal is greater than unity (|slope| > 1) and therefore the behaviour is chaotic. The character of the return map is also very similar to that of Buchler & Kolláth (2011) (see their fig. 3) who studied the 9:2 resonance suspected to cause the Blazhko effect in RR Lyrae stars. Clearly the two half-integer resonances lead to similar types of dynamical behaviour, either to a strictly periodic modulation or to a chaotic one. We stress, however, that our models, both hydrodynamic and based on the integration of AEs, are not 'too chaotic' – the modulation may be described as quasi-periodic or more or less periodic. This is exactly what we observe in Blazhko RR Lyrae stars.

The evolution close to the saddle point, in particular the differences in periods of the consecutive modulation cycles, can be understood through analysis of the flow field, that is, $(\dot{A}, \dot{B})$, which varies with time. It is tangent to the trajectory at the point $(A(t), B(t))$. The animation available as Supporting Information with the online version of the article shows the evolution for two trajectories: one located closer to the saddle than the other. A snapshot from this animation is plotted in Fig. 14. It is clear that the saddle trajectories are at first attracted, but repelled later on. Also the evolution at the saddle is slow (short vectors in the flow field) – the closer to the saddle, the slower the evolution. Thus, the modulation cycles corresponding to the two trajectories have different length.

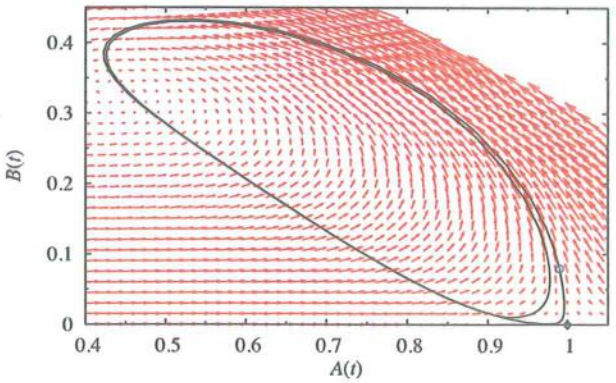

Figure 14. Snapshot from the animation available as Supporting Information with the online version of the article. Trajectories for two modulation cycles passing either close to or farther away from the saddle are plotted. The flow field is visualized at the instant marked with the circle.

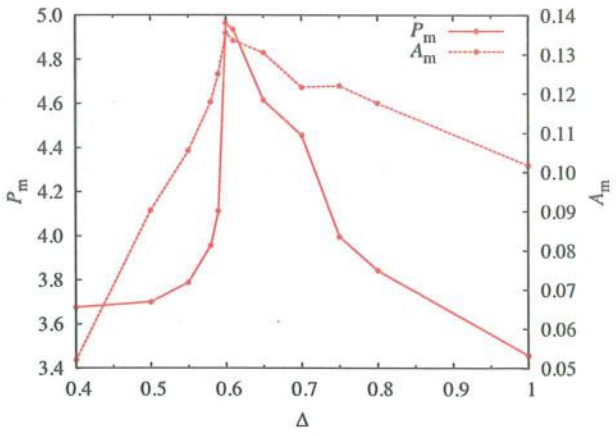

Figure 15. Mean modulation periods and modulation amplitudes as a function of Δ.

In Fig. 15 we plot the mean modulation periods and modulation amplitudes, as defined in Section 2.1, for a set of models with different Δ. Just as in the case of the hydrodynamic models (with 120 and 128 $L_\odot$, see Fig. 5), we observe the increase of the mean modulation period, accompanied by the increase of the modulation

amplitude. The longest modulation period is found for $\Delta = 0.6$ for which the modulation is chaotic.

4 DISCUSSION

(i) *Origin of the period doubling and modulation of pulsation.* In Fig. 1, loci of several half-integer resonances are plotted. In principle, each of them may cause the period-doubling effect, provided that the resonant mode is not damped too strongly, and that the respective model falls close to the resonant centre (Moskalik & Buchler 1990). These conditions rule out all the resonances displayed in Fig. 1 except the 3:2 resonance between the fundamental mode and the first overtone. In Fig. 16, we plot the amplitude of the period doubling (amplitude of the highest peak at around $f_0/2$) versus the mismatch parameter for the three half-integer resonances. Only models with $136\,L_\odot$ are plotted as for this luminosity we conducted a model survey through the full period-doubling domain.

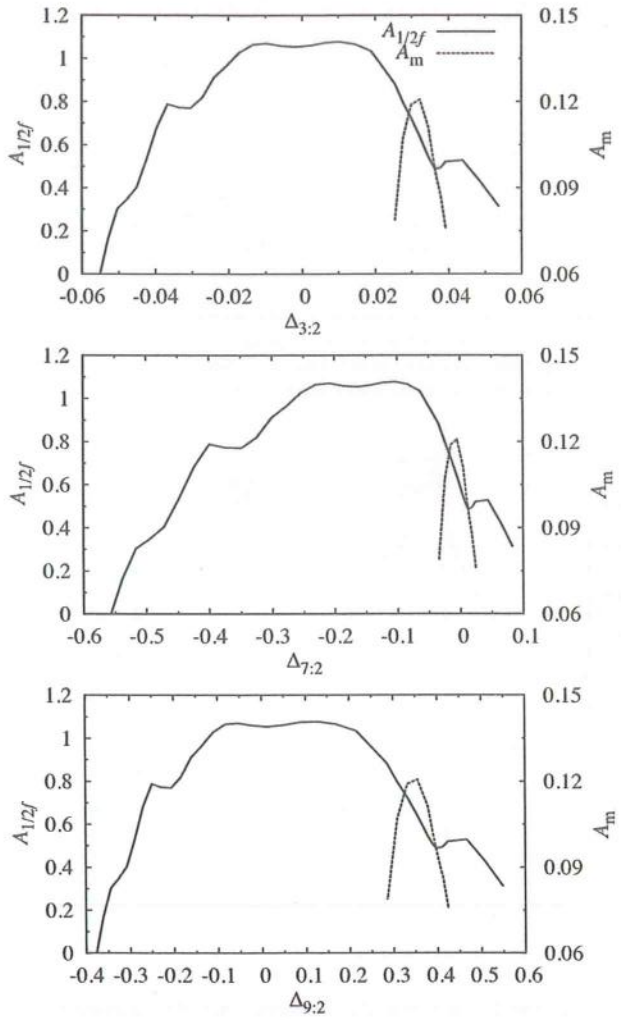

Figure 16. Amplitude of the subharmonic frequency, $A_{1/2f}$, and amplitude of the highest modulation peak at f_0, A_m, plotted versus the mismatch parameters for the 3:2 resonance with the first overtone, $\Delta_{3:2} = \omega_1/\omega_0 - 1.5$ (top panel), 7:2 resonance with the fourth overtone, $\Delta_{7:2} = \omega_4/\omega_0 - 3.5$ (middle panel) and 9:2 resonance with the seventh overtone, $\Delta_{9:2} = \omega_7/\omega_0 - 4.5$ (bottom panel).

It is clear that only for the 3:2 resonance are all the models close to the resonance centre, with $|\Delta_{3:2}| < 0.06$ (where $\Delta_{3:2} = \omega_1/\omega_0 - 1.5$). Considering, for example, the 7:2 resonance with the fourth overtone (middle panel of Fig. 16), although some models are located in the direct proximity of the resonance centre, other models within the period-doubling domain may be located as far as $|\Delta_{7:2}| > 0.5$, which rules out this resonance as a possible cause of period doubling. The same holds for the 9:2 resonance with the seventh overtone.

The domain with modulation of pulsation lies within the period-doubling domain. Its location with respect to the mismatch parameters is also plotted in Fig. 16, in which we used the amplitude of the highest modulation peak in the vicinity of f_0 ($f_0 + f_m$ or $f_0 - f_m$) to characterize the strength of modulation. For clarity, only the domain for $L = 136\,L_\odot$ is plotted; the domains for other luminosities fall roughly at the same location. From Fig. 1 it is clear that the domain with modulation of pulsation follows (at lower luminosities) the loci of the 7:2 resonance with the fourth overtone. Indeed, in Fig. 16 the resonance centre falls in the middle of the modulation domain and all of the models lie in close proximity to the resonance centre – as one may read from Fig. 16 ($|\Delta_{7:2}| < 0.05$ for all the models). This is, however, true also for the 3:2 resonance that causes the period-doubling effect. Although the models are offset with respect to the resonance centre, they all fall within $0.02 < \Delta_{3:2} < 0.04$. As the modulation domain arises within the period-doubling domain, which is caused by the 3:2 resonance, it is therefore natural to assume that the same resonance causes the modulation. It is confirmed from the analysis of the AEs presented in Section 3 (and also in Buchler & Kolláth 2011). No additional resonance is needed to cause the modulation. It appears within the period-doubling domain, not at its centre but at positive Δ (Fig. 15; note a different definition of Δ in this plot). Note that the positive mismatch as defined in equation (3) in Section 3 corresponds to $\Delta_{3:2} > 0$, just as we have for our hydrodynamic models (Fig. 16). Taking into account that all the behaviours we have found in our hydrodynamic models (period doubling, periodic and quasi-periodic modulation) can be reproduced with AEs for the 3:2 resonance only, we conclude that this resonance is the only cause of both period doubling and amplitude modulation in our hydrodynamic models.

(ii) *Reliability of the computed models.* Our models have strongly decreased eddy viscosity as compared to the standard models of BL Her stars, that is, $\alpha_m = 0.05$ compared to the $\alpha_m = 0.2$ we used in Smolec et al. (2012). Consequently, the pulsation is violent and spurious spikes appear in the luminosity curve. Still the models may represent the phenomena that may occur in real BL Her stars. Certainly it is so for the period doubling discovered in these stars only recently, 20 years after the effect was predicted based on hydrodynamic models (see the Introduction). No modulation of pulsation has been observed in BL Her stars so far.

The turbulent convection model that we use (Kuhfuß 1986) is a very simple 1D formula with several free parameters. The treatment of viscous effects seems to be the weakest point of this and similar models, which is not surprising. The viscous dissipation of turbulent energy takes place over many length-scales and its one-parameter description is, out of necessity, provisional. We note that the current convective models cannot reproduce a double-mode pulsation unless unphysical neglect of negative buoyancy below the convective zone leads to artificial viscous damping there (Smolec & Moskalik 2008b, 2010). With the purely radiative models, double-mode pulsation could not be reproduced either, unless artificial dissipation (replaced in convective codes by viscous dissipation) was decreased (Kovács & Buchler 1993). Similarly, the period doubling

in RR Lyrae models of Kolláth et al. (2011) was produced assuming lower values of eddy viscosity. Thus, the discovery of modulation of pulsation in BL Her stars cannot be excluded in the future.

(iii) *Models with chaotic modulation of pulsation.* In the case of $L = 136\,L_{\odot}$ we computed additional models across the IS. This allowed us to detect another domain in which pulsation is modulated, this time, however, in a very chaotic manner. In these models, we observe a wealth of dynamical behaviours. In particular, we identify several stability windows within the chaotic regime, with stable period k cycles (e.g. with $k = 3$, 7 or 9). They arise due to the tangent bifurcation and, as the control parameter ($T_{\rm eff}$) is increased, they undergo a series of pitchfork bifurcations (subharmonic cascade). These models will be subject of a separate paper (Smolec & Moskalik, in preparation).

5 IMPLICATIONS FOR THE BLAZHKO EFFECT IN RR LYRAE STARS

Modulation of pulsation is a common property of RR Lyrae stars, where it is called the Blazhko effect. In several stars, period doubling was also detected and was reproduced by the hydrodynamic RR Lyrae models of Kolláth et al. (2011), which, however, show no trace of modulation. Period doubling in the hydrodynamic RR Lyrae models is caused by the 9:2 resonance between the fundamental mode and the ninth overtone. The analysis of AEs by Buchler & Kolláth (2011) shows that the same resonance may cause modulation of pulsation. Confirmation of this result through direct hydrodynamic modelling would strongly support this radial resonance model. Our hydrodynamic BL Her models are the first models that demonstrate that the mechanism may indeed work. Except for larger luminosities, BL Her stars are siblings of RR Lyrae stars. The resonance that causes modulation of pulsation in our models, 3:2 resonance with the first overtone, cannot work in the case of RR Lyrae stars. Its locus falls beyond the RR Lyrae IS. It is clear, however, that the underlying dynamics are the same for the 3:2 and 9:2 resonances as studies of AEs indicate (Section 3 and Buchler & Kolláth 2011).

The great advantage of the radial resonance model is that it can cause the irregular modulation observed in Blazhko RR Lyrae stars. Striking evidence comes from the nearly continuous observations of the satellite missions (see e.g. Benkő et al. 2010; Guggenberger et al. 2012). Our models together with the analysis of AEs demonstrate how these irregularities may arise in the framework of the resonance model. For some model parameters, the modulation is no longer strictly periodic, but becomes chaotic. The models indicate that it happens when amplitudes of the involved fundamental and first overtone modes approach the unstable saddle point which corresponds to single periodic fundamental mode pulsation. Then, the period doubling is quenched and the variation of the modal amplitudes is very slow: the closer to the saddle, the slower the modulation. Thus, consecutive modulation cycles differ. It is worth noting that our models showing irregular modulation of pulsation reproduce other features of Blazhko RR Lyrae stars that simultaneously show the period-doubling effect. We observe qualitatively the same properties of Fourier spectra at half-integer frequencies – bunches of peaks, indicating the irregular nature of the period-doubling phenomenon, as well as swapping of higher/lower maximum cycles during the modulation (Szabó et al. 2010; Kolenberg et al. 2011; Molnár et al. 2012).

Comparison of the properties of modulation in our BL Her models to that observed in the Blazhko RR Lyrae stars points to the possible challenges for the radial resonance model. One of them is a very strong period-doubling effect in all our models. In contrast, only in a few Blazhko stars observed with satellite missions was the effect detected and its amplitude is rather low (Szabó et al. 2010). The strong period-doubling effect is also evident in our models based on the AEs integration, as well as in models corresponding to the 9:2 resonance analysed by Buchler & Kolláth (2011), which should be operational in RR Lyrae stars. The lack of period doubling in most of the Blazhko stars indicates that the modulation affects predominantly the fundamental mode, while the amplitude of the suspected resonant mode must remain quenched during most of the modulation cycle. Our models indicate that the period doubling is quenched while the model evolves close to the single-mode saddle point, where the amplitude of the resonant mode approaches zero. The resonant mode will always be modulated in the resonant scenario – the modal amplitudes must encircle the unstable two-mode fixed point – see Fig. 12. To decrease the modulation of the resonant mode and hence to quench the period doubling, one has to bring the two-mode fixed point closer to the $B(t) = 0$ axis. An extensive parameter study of the AEs is needed to point under which conditions such modulation is possible.

Irregularities are often detected in the Blazhko stars. In our models, they seem to be restricted to a very narrow parameter range; most of our models show a strictly periodic modulation. This might not be a problem for the resonant scenario if one takes into account the dispersion of stellar parameters (masses, luminosities, metallicities) of real stars or if one allows other resonances to play a dynamical role. The latter possibility is worth considering. Nearly 50 per cent of RR Lyrae stars (pulsating in the fundamental mode) show the Blazhko effect (Jurcsik et al. 2009; Benkő et al. 2010). It seems unlikely that the same, high-order resonance operates in all these stars. All other resonances within the radial modes face the same problems (or even harder, as most of the overtones are heavily damped). The half-integer resonances with non-radial modes may present a solution. Non-radial modes are densely packed in between the radial modes; thus, there is always a candidate for resonant coupling. On the other hand, mode selection would be a crucial problem here. We note that in recent years non-radial modes were detected in several RR Lyrae stars, both in ground-based and in space-based observations (e.g. Gruberbauer et al. 2007; Olech & Moskalik 2009; Guggenberger et al. 2012).

ACKNOWLEDGMENTS

We are grateful to Katrien Kolenberg for reading and commenting on the manuscript. This research has been supported by the Polish National Science Centre (DEC-2011/01/M/ST9/05914). Model computations presented in this paper were conducted on the PSK computer cluster in the Copernicus Centre, Warsaw, Poland.

REFERENCES

Asplund M., Grevesse N., Sauval A. J., Allende Prieto C., Kiselman D., 2004, A&A, 417, 751
Benkő J. et al., 2010, MNRAS, 409, 1585
Bergé P., Pomeau Y., Vidal C., 1984, Order within Chaos: Towards a Deterministic Approach to Turbulence. John Wiley & Sons, New York
Blazhko S., 1907, Astron. Nachr., 175, 325
Bono G., Marconi M., Stellingwerf R. F., 2000, A&A, 360, 245
Buchler J. R., Buchler N. E. G., 1994, A&A, 285, 213
Buchler J. R., Goupil M.-J., 1984, ApJ, 279, 394
Buchler J. R., Kolláth Z., 2011, ApJ, 731, 24
Buchler J. R., Moskalik P., 1992, ApJ, 391, 736
Buchler J. R., Moskalik P., Kovács G., 1990, ApJ, 351, 617

Feuchtinger M., Buchler J. R., Kolláth Z., 2000, ApJ, 544, 1056
Gruberbauer M. et al., 2007, MNRAS, 379, 1498
Guggenberger E., Kolenberg K., Chapellier E., Poretti E., Szabó R., Benkő J. M., Paparó M., 2011, MNRAS, 415, 1577
Guggenberger E. et al., 2012, MNRAS, 424, 649
Jurcsik J. et al., 2009, MNRAS, 400, 1006
Kienzle F., Moskalik P., Bersier D., Pont F., 1999, A&A, 341, 818
Klapp J., Goupil M. J., Buchler J. R., 1985, ApJ, 296, 514
Kolenberg K., 2008, J. Phys.: Conf. Ser., 118, 012060
Kolenberg K. et al., 2006, A&A, 459, 577
Kolenberg K. et al., 2010, ApJ, 713, L198
Kolenberg K. et al., 2011, MNRAS, 411, 878
Kolláth Z., Molnár L., Szabó R., 2011, MNRAS, 414, 1111
Kovács G., 2009, in Guzik J. A., Bradley P. A., eds, AIP Conf. Ser. Vol. 1170, Stellar Pulsation: Challenges for Theory and Observation. Am. Inst. Phys., New York, p. 261
Kovács G., Buchler J. R., 1989, ApJ, 346, 898
Kovács G., Buchler J. R., 1993, ApJ, 404, 765
Kuhfuß R., 1986, A&A, 160, 116
Molnár L., Kolláth Z., Szabó R., 2012a, MNRAS, 424, 31
Molnár L., Kolláth Z., Szabó R., Bryson S., Kolenberg K., Mullally F., Thompson S. E., 2012, ApJ, submitted
Moskalik P., Bucher J. R., 1990, ApJ, 355, 590
Moskalik P., Bucher J. R., 1993, Ap&SS, 210, 301
Nowakowski R., 2005, Acta Astron., 55, 1
Olech A., Moskalik P., 2009, A&A, 494, L17
Seaton M., 2005, MNRAS, 362, L1
Simon N. R., Schmidt E. G., 1976, ApJ, 205, 162
Smolec R., Moskalik P., 2008a, Acta Astron., 58, 193
Smolec R., Moskalik P., 2008b, Acta Astron., 58, 233
Smolec R., Moskalik P., 2010, A&A, 524, A40
Smolec R., Moskalik P., Kolenberg K., Bryson S., Cote M. T., Morris R. L., 2011, MNRAS, 414, 2950
Smolec R. et al., 2012, MNRAS, 419, 2407
Soszyński I. et al., 2011, Acta Astron., 61, 285
Stellingwerf R. F., 1974, ApJ, 192, 139
Stothers R. B., 2006, ApJ, 652, 643
Szabados L., 2010, in Sterken C., Samus N., Szabados L., eds, Variable Stars, the Galactic Halo and Galaxy Formation. Sternberg Astronomical Institute of Moscow University, Russia, p. 37
Szabó R. et al., 2010, MNRAS, 409, 1244
Wallerstein G., 2002, PASP, 114, 689

SUPPORTING INFORMATION

Additional Supporting Information may be found in the online version of this article:

Animation. Model evolution in the $B(t)$ versus $A(t)$ plane ($\Delta = 0.6$) for the two modulation cycles. The diamond marks the location of the unstable single-mode fixed point (saddle). The circle shows the model's position during the evolution. The instantaneous flow field $(\dot{A}(t), \dot{B}(t))$ is plotted with vectors. A snapshot from the animation is plotted in Fig. 14.

Please note: Wiley-Blackwell are not responsible for the content or functionality of any supporting materials supplied by the authors. Any queries (other than missing material) should be directed to the corresponding author for the article.

This paper has been typeset from a TEX/LATEX file prepared by the author.